Generation of maximally-polarization-entangled photons on a chip

Sergei V. Zhukovsky,[1,2,*] Lukas G. Helt,[1] Dongpeng Kang,[2] Payam Abolghasem,[2] Amr S. Helmy,[2] and J. E. Sipe[1]

[1]*Department of Physics and Institute for Optical Sciences, University of Toronto, 60 St. George Street, Toronto, Ontario, Canada M5S 1A7*

[2]*The Edward S. Rogers Department of Electrical and Computer Engineering, University of Toronto, 10 King's College Road, Toronto, Ontario, Canada M5S 3G4*

(Received 1 September 2011; published 25 January 2012)

We propose a method of generating maximally-polarization-entangled states by type-II spontaneous parametric down-conversion in Bragg reflection waveguides. Analytic expressions for the group velocities of down-converted modes are used to engineer zero group-velocity mismatch at the operating point, making the spectra of photons within a down-converted pair indistinguishable and thus leading to a maximally-polarization-entangled state. The results can be used for the creation and manipulation of polarization-entangled qubits entirely on a chip.

DOI: 10.1103/PhysRevA.85.013838 PACS number(s): 42.65.Lm, 03.67.Bg, 42.82.Et, 78.20.Fm

I. INTRODUCTION

Entanglement is the enabling phenomenon behind aspects of quantum communication and information processing such as quantum cryptography, dense coding, teleportation, and the design of quantum logic elements [1–3]. It is also a crucial physical phenomenon for testing the fundamentals of quantum theory, e.g., the violation of Bell's inequalities. Entangled photons are particularly appealing for communication applications and can be easily generated by spontaneous parametric down-conversion (SPDC) in $\chi^{(2)}$-nonlinear crystals [2].

Photons can be entangled in different degrees of freedom (DOFs), including energy, momentum, polarization, and time of arrival. Among these, polarization-entangled photon pairs are the most studied [4], as they are the most accessible and controllable; two orthogonal polarizations of a photon form a two-state quantum system or qubit. Single and entangled qubits are key elements in linear quantum computing, which would make previously intractable problems in cryptography [5] and quantum chemistry [6] computationally feasible. Polarization-entangled qubits have also been used in demonstrations of quantum teleportation [7].

To date, most experiments involve photons propagating in free space and circuits made of bulk optical elements. Unfortunately, their large size, need for precise alignment, and sensitivity to environmental factors seriously limit the practical aspect of photonic quantum technologies [8]. The ability to bring quantum computing and information processing experiments from an optical table to an optical chip would therefore constitute a major breakthrough in the field. Recently, there has been considerable success in that area along two directions. One of them is the design of on-chip quantum-interference circuits [2,5,9]. The other is the advances in the design of SPDC-based entangled photon sources suitable for on-chip integration [10–12]. However, the next step of integrating such an entangled photon source with a quantum circuit on a single optical chip has not yet been taken, although fabrication appears to be feasible [13].

The design of polarization-entangled photon sources on a chip is hampered by the influence of form birefringence (see, e.g., Ref. [14]), leading to different velocities for differently polarized photons and to unwanted polarization changes to an arbitrarily polarized photon under propagation. Birefringence also causes the generated photons to become hyperentangled in both polarization and time-energy [15], so that it becomes impossible to factorize their state into functions describing entanglement in separate DOFs. While this property may be desirable in some contexts [16,17], the mainstream approach is to eliminate the mutual dependence between entanglement in the two DOFs, so that no information about a photon's polarization can be inferred from its spectral properties [18]. Although there are methods to achieve this indistinguishability by off-chip postcompensation [19], material and form birefringence still pose a fundamental hindrance to designing a source of polarization-entangled photon pairs integrated on a chip compatible with a mature semiconductor fabrication platform. Such a source would be highly desirable for on-chip quantum optical applications

In this paper, we propose a means to generate maximally-polarization-entangled photon pairs in integrated optical waveguides by introducing a universal method of form-birefringence cancellation. Unlike earlier approaches [20,21], the group (rather than phase) velocity of differently polarized down-converted photons is made to coincide, so that the state of generated photons becomes factorizable with respect to frequency and polarization DOFs. We use modal phase matching (PM) in Bragg reflection waveguides (BRWs) [22] to make birefringence control independent of the PM conditions. The proposed method extends the available geometries for birefringence-free waveguides beyond simple square [2,5] or circular cross sections [9], thus making such waveguides much more compatible with semiconductor fabrication platforms. As an example, we propose an $Al_xGa_{1-x}As$-BRW structure phase matched for type-II SPDC near 1550 nm. For both picosecond and femtosecond pump pulses, we examine the state of generated photons, and show that they have maximal polarization entanglement.

In addition to being technologically mature, the $Al_xGa_{1-x}As$ fabrication platform features a strong $\chi^{(2)}$ nonlinearity, a broad transparency window, and a wide range of refractive index variation. Given the recent experimental observation of SPDC [12] and the realization of monolithic integration with a diode pump laser [13], combined with ongoing development of quantum interference circuitry on a chip [2,9], our results identify a route to fully on-chip creation

*szhukov@physics.utoronto.ca

and manipulation of polarization qubits. Our results can also have other uses in photonic quantum technology, such as improving the efficiency of optical memory readouts [23,24].

The paper is organized as follows. In Sec. II, we present our method for achieving similar group velocity in orthogonally polarized waveguide modes in the presence of form birefringence. We outline the use of such modes as down-converted modes in type-II SPDC, and present an example design based on a BRW structure. In Sec. III, we calculate the joint spectral intensity of generated photon pairs. Our waveguide source leads to states that are much closer to being maximally polarization entangled than in sources previously proposed for on-chip applications. Finally, we summarize in Sec. IV.

II. GROUP VELOCITY MATCHING IN THE PRESENCE OF FORM BIREFRINGENCE

We first consider a slab dielectric waveguide where the core layer has refractive index n_c and thickness t_c, surrounded by an infinitely extended cladding with index $n_o < n_c$ [Fig. 1(a)]. Modes guided in the core due to total internal reflection (TIR) can have either TE (H) or TM (V) polarization. Their effective indices $n_{\text{eff}} = n_{\text{TE,TM}}$ are determined by the pole condition

$$1 - (r_{\text{TE,TM}})^2 \exp[2i w_{\text{TE,TM}} t_c \omega/c] = 0, \tag{1}$$

where $w_{\text{TE,TM}} = [n_c^2 - n_{\text{TE,TM}}^2(\omega)]^{1/2}$ with the square root chosen so that $\text{Im}\, w \geqslant 0$, and if $\text{Im}\, w = 0$, then $\text{Re}\, w \geqslant 0$; $r_{\text{TE,TM}}$ is the standard Fresnel reflection coefficient at the core-cladding interface. For $n_o < n_{\text{eff}} < n_c$, it takes the form of a polarization-dependent phase shift $r = e^{i\delta}$ written as

$$\delta_{\text{TE}} = f\left(2n_{\text{TE}}^2\right), \quad \delta_{\text{TM}} = f\left[\left(n_c^4 + n_o^4\right)n_{\text{TM}}^2/n_c^2 n_o^2\right],$$

where

$$f(x) = \arctan\left[-2\frac{\sqrt{\left(n_c^2 - n_{\text{TM}}^2\right)\left(n_{\text{TM}}^2 - n_o^2\right)}}{n_c^2 + n_o^2 - x}\right].$$

Equation (1) is the waveguide dispersion relation in implicit form; it allows us to find $n_{\text{TE,TM}}(\omega)$, albeit only numerically [25]. From this, the group velocity for the two modes, $v_{\text{TE,TM}} = c\{n_{\text{TE,TM}} + \omega[dn_{\text{TE,TM}}(\omega)/d\omega]\}^{-1}$, can be determined. In a general case, $r_{\text{TM}} \neq r_{\text{TE}}$ due to form birefringence, causing $n_{\text{TM}} \neq n_{\text{TE}}$ and, in turn, $\Delta v_g = v_{\text{TM}} - v_{\text{TE}} \neq 0$. However, we are aiming at a design where the group velocities for differently polarized down-converted photons are equal ($\Delta v_g = 0$).

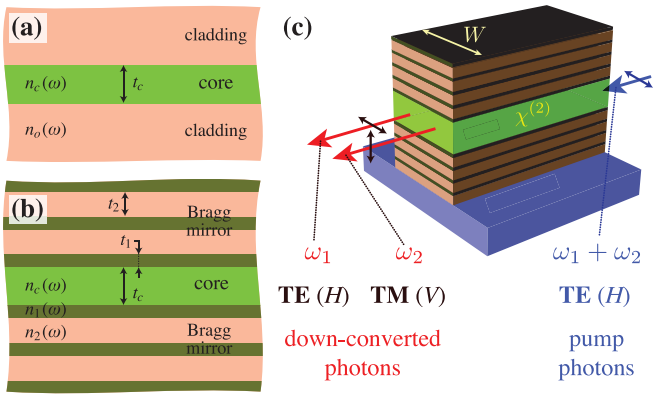

FIG. 1. (Color online) Schematic of a dielectric slab waveguide (a) without and (b) with refractive index modulation (Bragg mirror) in the cladding; (c) schematic of a 2D ridge BRW with type-II SPDC.

We note that the derivative $dn_{\text{TE,TM}}(\omega)/d\omega$ can be expressed as an algebraic function of $n_{\text{TE,TM}}(\omega)$ and ω. The effective index splitting between TE- and TM-polarized modes is small,

$$\Delta n_{\text{eff}} = n_{\text{TM}} - n_{\text{TE}} \ll n_{\text{TE,TM}}$$

and

$$\left(n_c^4 + n_o^4\right)/\left(n_c^2 n_o^2\right) \gtrsim 2.$$

Thus the expression for Δv_g can be Taylor expanded with respect to two small parameters, Δn_{eff} and

$$\Delta x = \frac{\left(n_c^4 + n_o^4\right)n_{\text{TM}}^2}{n_c^2 n_o^2} - 2n_{\text{TE}}^2.$$

This results in an analytic expression $\Delta v_g \equiv F(\omega, n_{\text{TE}})$, where n_{TE} should still be determined numerically. The function F can easily account for material dispersion in $n_{c,o}$, which is particularly important for semiconductors operating close to their band gap, such as $Al_xGa_{1-x}As$.

By looking at the function $F(\omega,n)$, where $n \in (n_o, n_c)$ is taken to be an arbitrary parameter rather than the actual value of the effective index, it is easy to verify that single-mode waveguides with small t_c cannot satisfy $\Delta v_g = 0$ since $F(\omega,n) > 0$ for all available n [Fig. 2(a)]. However, increasing the core thickness makes $F(\omega,n)$ cross zero and simultaneously increases n_{TE} [Fig. 2(a)]. Hence a slab waveguide for TIR-guided modes with $v_{\text{TE}} = v_{\text{TM}}$ at a given ω can be designed simply by choosing t_c in such a way that $F(\omega,n)$ crosses zero at $n = n_{\text{TE}}$.

For an SPDC process where these modes would carry down-converted photons, we need to phase match them with a pump

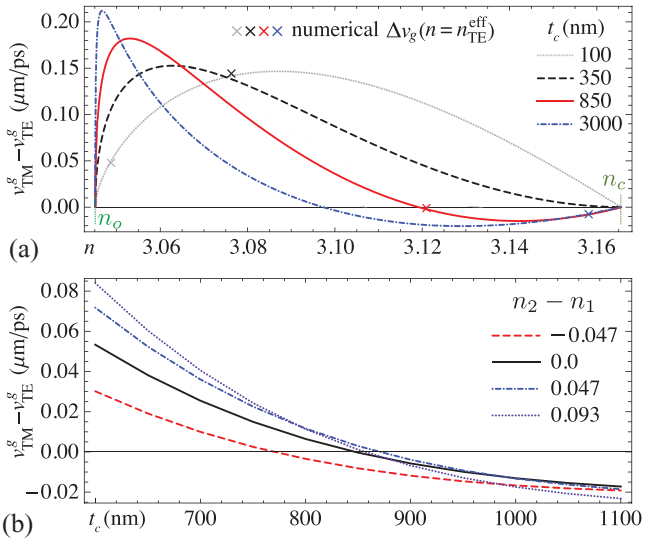

FIG. 2. (Color online) (a) The analytic dependence $\Delta v_g = F(\omega,n)$ at 1550 nm on n for different t_c (crosses denote numerically determined Δv_g at $n = n_{\text{TE}}$ for each t_c; it is seen that analytical and numerical results are in good agreement). (b) The dependence $\Delta v_g(t_c)$ for different index modulation depth ($n_2 - n_1$) in the Bragg cladding.

mode having the frequency $\omega_p = 2\omega$. To do so, we use a BRW structure [22] where the refractive index in the cladding is periodically modulated around n_o [see Fig. 1(b)]. In a BRW made of a highly dispersive material such as $Al_xGa_{1-x}As$, light at the wavelength $\lambda = 2\pi c/\omega$ is guided by TIR, whereas light at $\lambda/2 = 2\pi c/\omega_p$ is guided by Bragg reflection from the claddings. The geometrical parameters can be chosen so that $n_{\rm TE}(\omega) + n_{\rm TM}(\omega) = 2n_{\rm eff}(\omega_p)$ to achieve type-II SPDC, where a pump photon from the TE-polarized pump Bragg-guided mode will produce a pair of cross-polarized photons going into TE- and TM-polarized TIR-guided modes, which, as described above, have equal group velocity. To maximize the reflectivity of the Bragg claddings, the layer thicknesses should satisfy the quarter-wave (QW) condition [26]

$$t_1\sqrt{n_1^2 - n_{\rm eff}^2(\omega_p)} = t_2\sqrt{n_2^2 - n_{\rm eff}^2(\omega_p)} = (\lambda/2)/4 \equiv \Lambda. \quad (2)$$

Note that since $\Delta v_g = 0$ requires large values of t_c, the fundamental Bragg mode, for which $w_c t_c \simeq \Lambda$, cannot be phase matched at the desired $n_{\rm eff}$. We use the higher-order Bragg mode with $w_c t_c \simeq 3\Lambda$, which can be phase matched.

Modulation in the cladding certainly changes the expressions for r and δ; however, they can still be evaluated either numerically (by using the transfer matrix methods) or semianalytically (by using the recurrent Airy formulas for the reflection coefficients of multilayers [27]). Figure 2(b) shows the influence of the modulation depth $(n_2 - n_1)$ on Δv_g. It can be seen that a point where $\Delta v_g = 0$ can still be reached by adjusting t_c. The resulting example of a one-dimensional (1D) design for $(x_c, x_1, x_2) = (0.4, 0.6, 0.7)$ has $(t_c, t_1, t_2) = (755, 209, 279)$ nm. The corresponding phase matching (PM) diagrams are shown in Fig. 3(a).

To facilitate using the resulting SPDC-capable waveguide on an optical chip, the proposed design principles must be applied to the 2D ridge-waveguide geometry [see Fig. 1(c)]. As the finite ridge width is known to have a positive contribution

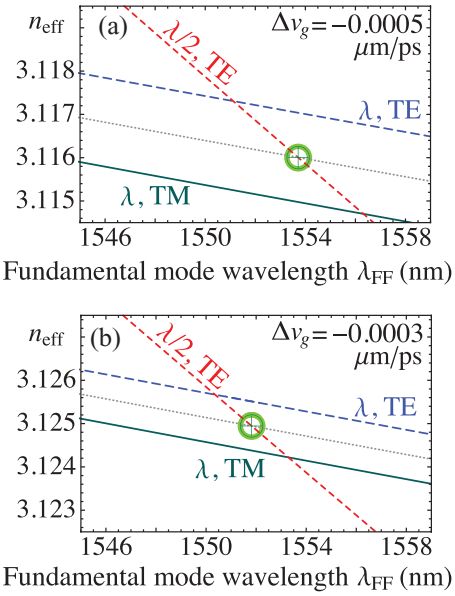

FIG. 3. (Color online) Mode dispersion diagrams showing type-II PM in BRWs with $\Delta v_g = 0$: (a) 1D slab and (b) 2D ridge ($W = 4.4\,\mu$m), obtained in a vectorial commercial mode solver [28].

to Δv_g, a slab waveguide should be deliberately designed to operate at $\Delta v_g < 0$. Cladding layer thicknesses $t_{1,2}$ need to be slightly increased to maintain PM near the desired λ. The resulting design for the ridge width $W = 4.4\,\mu$m has $(t_c, t_1, t_2) = (1014, 232, 341)$ nm. Its PM diagrams are shown in Fig. 3(b). It can be seen that near-zero Δv_g is indeed achieved.

III. POLARIZATION ENTANGLEMENT IN GENERATED BIPHOTONS

We follow our earlier work [29,30] to determine the state of generated photons. The input is a coherent state $|\psi_{\rm in}\rangle = \exp[\mu \int d\omega \phi_p(\omega) a^{p\dagger}_{\sigma\omega} - {\rm H.c.}]|{\rm vac}\rangle$. The pump pulse envelope is $\phi_p(\omega) \propto \exp[-(\omega - \omega_p)^2/\Omega^2]$, which we take to describe a pulse with center frequency ω_p and intensity full width at half maximum $2\sqrt{2\ln 2}/\Omega = 1.8$ ps. We use the interaction Hamiltonian

$$H = \sum_{\alpha\beta\gamma} \int d\omega_1 d\omega_2 d\omega S_{\alpha\beta\gamma}(\omega_1, \omega_2, \omega) a^{d\dagger}_{\alpha\omega_1} a^{d\dagger}_{\beta\omega_2} a^{p}_{\gamma\omega} + {\rm H.c.} \quad (3)$$

to calculate the state of the generated photons in the limit of low probability of pair production per pump pulse ($|\nu|^2 \ll 1$),

$$|\psi_{\rm gen}\rangle \approx (1 + \nu C^\dagger_{\rm II})|{\rm vac}\rangle, \quad (4)$$

with the two-photon creation operator

$$C^\dagger_{\rm II} = \frac{1}{\sqrt{2}} \sum_{\alpha,\beta} \int_0^\infty d\omega_1 d\omega_2 \phi_{\alpha\beta}(\omega_1, \omega_2) a^{d\dagger}_{\alpha\omega_1} a^{d\dagger}_{\beta\omega_2}. \quad (5)$$

Greek subscripts denote polarization components; $a^p_{\sigma\omega}$ and $a^d_{\sigma\omega}$ are boson mode operators for pump and down-converted photons, respectively, with frequency ω and polarization σ, obeying the commutation relations $[a^m_{\sigma\omega}, a^{m'\dagger}_{\sigma'\omega'}] = \delta_{mm'}\delta_{\sigma\sigma'}\delta(\omega - \omega')$ for $m, m' = p, d$. The function $\phi_{\alpha\beta}(\omega_1, \omega_2) = \phi_{\beta\alpha}(\omega_2, \omega_1)$ is the biphoton wave function (BWF)

$$\phi_{\alpha\beta}(\omega_1, \omega_2) \propto \phi_p(\omega_1 + \omega_2) {\rm sinc}\left(\Delta k^{\gamma\alpha\beta}_{\rm PM} L/2\right), \quad (6)$$

where

$$\Delta k^{\gamma\alpha\beta}_{\rm PM} = k^p_\gamma(\omega_1 + \omega_2) - k^d_\alpha(\omega_1) - k^d_\beta(\omega_2)$$

is defined by the PM conditions, and the mode dispersion relations around the PM frequency are taken as

$$k^{m=p,d}_\sigma = k^m_{\sigma 0} + (\omega - \omega_{m0})/v^m_\sigma + (\omega - \omega_{m0})^2 \Lambda^m_\sigma.$$

It can be seen that to a good approximation, the condition $\Delta v_g = v^d_{\rm TM} - v^d_{\rm TE} = 0$ results in

$$\phi_{\alpha\beta}(\omega_1, \omega_2) = \phi_{\alpha\beta}(\omega_2, \omega_1). \quad (7)$$

Indeed, Fig. 4 shows that $\phi_{HV}(\omega_1, \omega_2)$ for type-II SPDC lacks this symmetry in a general BRW, but acquires it in the design where $\Delta v_g = 0$. From Eq. (7), it follows that the type-II BWF in Eq. (5) takes the form (recall that TE $= H$, TM $= V$)

$$\phi_{\alpha\beta}(\omega_1, \omega_2) = [\delta_{\alpha,H}\delta_{\beta,V} + \delta_{\alpha,V}\delta_{\beta,H}]\xi(\omega_1, \omega_2), \quad (8)$$

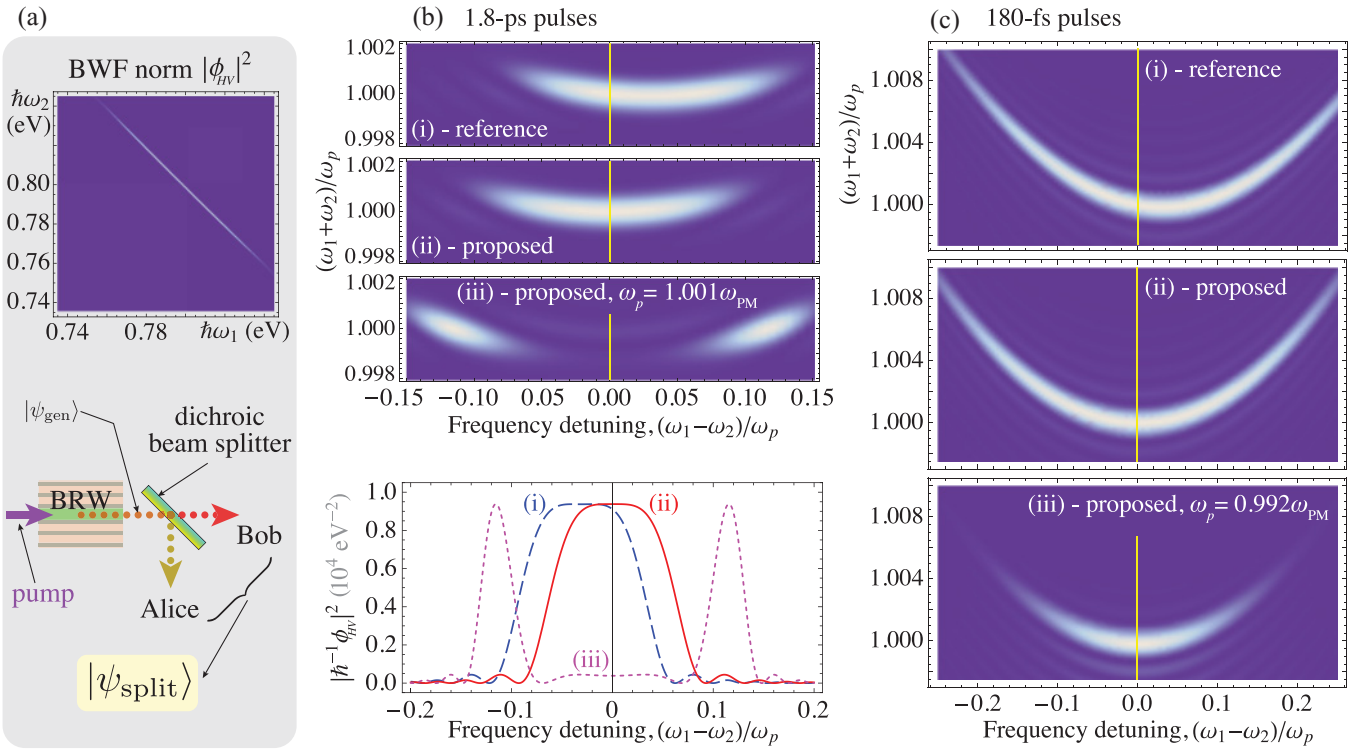

FIG. 4. (Color online) (a) Norm of a BWF, $|\phi_{HV}(\omega_1,\omega_2)|^2$, for the proposed design using picosecond (1.8 ps) pump pulses, with the schematic of turning the generated biphotons into a maximally-polarization-entangled state. (b) Comparison between BWFs for the reference BRW design of Ref. [31] with (i) $\Delta v_g \simeq 0.3\,\mu$m/ps, and the proposed BRW design of Fig. 3(b) with $\Delta v_g \approx 0$ pumped at the frequency of (ii) PM and (iii) 0.1% higher. The bottom plot shows the cross section of the BWF along the line $\omega_1 + \omega_2 = \omega_p$. (c) Same as (b), but for femtosecond (180 fs) pump pulses for (i) the reference BRW vs the proposed BRW pumped at (ii) ω_{PM} and (iii) 0.8% lower.

where $\xi(\omega_1,\omega_2) = \xi(\omega_2,\omega_1)$. The state of biphotons generated in type-II SPDC are, from Eqs. (4) and (5),

$$\begin{aligned}|\psi_{pair}\rangle &= \frac{1}{\sqrt{2}}\int_0^\infty [\phi_{HV}(\omega_1,\omega_2)\,|\omega_1 H;\omega_2 V\rangle \\ &\quad + \phi_{VH}(\omega_1,\omega_2)\,|\omega_1 V;\omega_2 H\rangle]\,d\omega_1 d\omega_2 \\ &= \frac{1}{\sqrt{2}}\int_0^\infty d\omega_1 d\omega_2 \xi(\omega_1,\omega_2)\,[|\omega_1 H;\omega_2 V\rangle \\ &\quad + |\omega_1 V;\omega_2 H\rangle]\,, \end{aligned} \tag{9}$$

where $|\omega\sigma\rangle = a^{d\dagger}_{\sigma\omega}|\text{vac}\rangle$.

A usable polarization-entangled state can be achieved probabilistically using a beam splitter to send one photon of the pair to Alice and one to Bob [32]. Better yet, the frequency DOF can be used to separate the high-frequency ($\omega > \omega_p/2$) and the low-frequency ($\omega < \omega_p/2$) photon in each pair and send them to Alice and Bob, respectively [Fig. 4(a)]. Such frequency separation can be implemented on a chip by using elements with engineered spectral properties, such as directional couplers or add-drop filters. Using Eqs. (4) and (5) with Eq. (8), and assuming the model of an idealized dichroic beam splitter, the state of each pair is

$$\begin{aligned}|\psi_{split}\rangle \propto \int_0^{\omega_p/2} d\omega_1 \int_{\omega_p/2}^\infty d\omega_2 \xi(\omega_1,\omega_2) \\ \times\,[|\omega_1 H;\omega_2 V\rangle + |\omega_1 V;\omega_2 H\rangle]\,. \end{aligned} \tag{10}$$

Due to the integration limits, the form $|\psi_A;\psi_B\rangle$ in Eq. (10) can be interpreted as ψ_A denoting Alice's photon and ψ_B denoting Bob's photon. We see that the polarization and frequency DOFs are separated, so it is impossible to tell the polarization of a photon sent to Alice (or Bob) by looking at its frequency information.

To quantify the degree of polarization entanglement, it is convenient to define [33]

$$G = \int d\omega_1 d\omega_2 \phi_{HV}(\omega_1,\omega_2)\phi^*_{VH}(\omega_1,\omega_2). \tag{11}$$

The case when G attains its maximum value ($G = G^* = 1$) corresponds to the maximum visibility in Hong-Ou-Mandel-type experiments involving down-converted photons [18] and maximum violation of Bell-type inequalities [4]. Hence, we will call the biphotons that conform to $G = G^* = 1$ *maximally* polarization entangled.

Our calculation shows that the proposed design [Figs. 3(b) and 4(b)] has $1 - G = 1.6 \times 10^{-6}$, as opposed to $1 - G = 0.463$ for a reference BRW with nonzero Δv_g [Fig. 4(b)]. Choosing ω_p slightly above the PM condition produces a BWF that is small near $\omega_p/2$ [see Fig. 4(b)]. This results in $1 - G = 7.2 \times 10^{-6}$, which is similarly very small, and makes the frequency separation easier and much less susceptible to the effects of a nonideal beam splitter.

Given the recent progress in generating ultrafast pulses of entangled photons with high brightness using cavity enhancement [34], and the advent of fast and efficient time-resolved detectors (see Ref. [35] and references therein), it is of interest to investigate how the proposed source would function in

the femtosecond time range. The corresponding BWFs are shown in Fig. 4(c). It can be seen that the down-conversion bandwidth is substantially increased. The dominant feature in the BWF becomes the curvature in the sinc function in Eq. (6), defined by the group-velocity dispersion in the down-converted modes Λ^d. Nonzero group-velocity mismatch Δv_g makes this curvature asymmetric, which not only diminishes the degree of polarization entanglement, but also reduces the effectiveness of spectral filtering to remedy this. However, bringing Δv_g close to zero restores the symmetry in Eq. (7) even in the femtosecond case. Quantitatively, $1 - G$ is seen to decrease from 0.826 for the reference BRW all the way down to 2×10^{-5} for the proposed structure. Shifting the pump frequency ω_p slightly below PM greatly reduces the SPDC bandwidth at the cost of lowered pair-generation efficiency, and keeps $1 - G$ very small (9.1×10^{-6}).

It was shown earlier [33] that polarization entanglement in the generated states can only be reliably swapped if the function on the right-hand side of Eq. (8) is separable, i.e., if $\xi(\omega_1,\omega_2) = \zeta(\omega_1)\zeta(\omega_2)$. The BWFs in Fig. 4 show a marked anticorrelated character and clearly do not satisfy this condition. This limits the applicability of the proposed source for long-distance quantum communication. However, the principles put forth in the present paper can be used with other waveguide designs where SPDC has a narrower bandwidth (see, e.g., Ref. [36]).

Finally, it is worth noting that by combining the proposed approach of reducing Δv_g with known techniques of reducing Δn_{eff} [20,21] through choosing a proper combination of the ridge width and t_c, one can design a waveguide where both type-II and type-I SPDC will be phase matched at the same wavelength. This will enable selective production of $|HV\rangle + |VH\rangle$-like and $|HH\rangle + |VV\rangle$-like photon pairs, paving the way toward on-chip generation of optical Bell states. Note also that higher-order Bragg modes used for the pump in the proposed design have an overlap integral with the down-converted modes that is about 100 times smaller than for the pump modes used in the reference BRW. This decreases the pair-production rate accordingly, to around 4×10^{-10} pairs per pump photon or 0.5×10^6 (pairs/s)/mW of the pump power. These performance figures are still comparable to previous results [37] and allow the experimental observation of photons from the proposed source with realistic values of intrinsic pump power of several milliwatts; the generation efficiency can be further improved with structure optimizations.

IV. CONCLUSIONS

In summary, we have theoretically demonstrated that maximally-polarization-entangled photon pairs can be generated on an optical chip by cancellation of form birefringence in dielectric waveguides. The group velocities of differently polarized down-converted photons are made equal, in turn making the BWF symmetric. An example design based on a BRW structure [22] made of $Al_xGa_{1-x}As$, phase matched for type-II SPDC near 1550 nm, has been proposed and investigated. The results obtained complement recent accounts of monolithically integrating an SPDC source with a diode pump laser [12,13], and are compatible with on-chip quantum-interference circuitry [2,5,9], paving the way for fully on-chip creation and manipulation of polarization qubits and Bell states. In addition, they have other uses in photonic quantum technologies, e.g., in a quantum readout for optical memory, where it has recently been shown that using nonclassical states (in particular, entangled) can substantially improve the readout efficiency [23].

ACKONOWLEDGMENT

This work was supported by the Natural Sciences and Engineering Research Council of Canada (NSERC).

[1] T. D. Ladd, F. Jelezko, R. Laflamme, Y. Nakamura, C. Monroe, and J. L. O'Brien, Nature (London) **464**, 45 (2010).
[2] J. L. O'Brien, A. Furusawa, and J. Vučković, Nature Photon. **3**, 687 (2009).
[3] N. Gisin, G. Ribordy, W. Tittel, and H. Zbinden, Rev. Mod. Phys. **74**, 145 (2002).
[4] K. Edamatsu, Jpn. J. Appl. Phys. **11**, 7175 (2007).
[5] M. G. Thompson, A. Politi, J. C. F. Matthews, and J. L. O'Brien, IET Circuits Devices Syst. **5**, 94 (2011).
[6] B. Lanyon, J. Whitfield, G. Gillett, E. Goggin, M. Almeida, I. Kassal, J. Biamonte, M. Mohseni, B. Powell, M. Barbieri, A. Aspuru-Guik, and A. White, Nature Chem. **2**, 106 (2010).
[7] D. Bouwmeester, J.-W. Pan, K. Mattle, M. Eibl, H. Weinfurter, and A. Zeilinger, Nature (London) **390**, 575 (1997).
[8] M. Lobino and J. O'Brien, Nature (London) **469**, 43 (2011).
[9] L. Sansoni, F. Sciarrino, G. Vallone, P. Mataloni, A. Crespi, R. Ramponi, and R. Osellame, Phys. Rev. Lett. **105**, 200503 (2010).
[10] A. De Rossi, V. Ortiz, and M. Calligaro, B. Vinter, J. Nagle, S. Ducci, and V. Berger, Semicond. Sci. Technol. **19**, L99 (2004).
[11] S. M. Spillane, M. Fiorentino, and R. G. Beausoleil, Opt. Express **15**, 8770 (2007).
[12] R. Horn, P. Abolghasem, B. Bijlani, A. S. Helmy, and G. Weihs, in *CLEO: 2011 Technical Digest* (Optical Society of America, Washington, DC, 2011), Report No. QThN2.
[13] B. Bijlani, P. Abolghasem, A. Reijnders, and A. S. Helmy, in *CLEO: 2011 Postdeadline Papers* (Optical Society of America, Washington, DC, 2011), Report No. PDPA3.
[14] A. S. Helmy, P. Abolghasem, J. S. Aitchinson, B. Bijlani, J. Han, B. M. Holmes, D. C. Hutchings, U. Younis, and S. J. Wagner, Laser Photon. Rev. **5**, 272 (2011).
[15] P. G. Kwiat, J. Mod. Opt. **44**, 2173 (1997).
[16] J. T. Barreiro, N. K. Langford, N. A. Peters, and P. G. Kwiat, Phys. Rev. Lett. **95**, 260501 (2005).
[17] C.-M. Li, K. Chen, A. Reingruber, Y.-N. Chen, and J.-W. Pan, Phys. Rev. Lett. **105**, 210504 (2010).

[18] W. P. Grice and I. A. Walmsley, Phys. Rev. A **56**, 1627 (1997).
[19] D. Branning, W. P. Grice, R. Erdmann, and I. A. Walmsley, Phys. Rev. Lett. **83**, 955 (1999).
[20] K. S. Chang and W. P. Wong, IEEE J. Quantum Electron. **35**, 1554 (1999).
[21] W. P. Wong and K. S. Chang, IEEE J. Quantum Electron. **37**, 1138 (2001).
[22] A. S. Helmy, Opt. Express **14**, 1243 (2006).
[23] S. Pirandola, Phys. Rev. Lett. **106**, 090504 (2011).
[24] R. Nair, Phys. Rev. A **84**, 032312 (2011).
[25] H. Kogelnik, in *Integrated Optics: Topics on Applied Physics* (Springer, Berlin, 1972), Vol. 7, pp. 13–81.
[26] B. R. West and A. S. Helmy, IEEE J. Sel. Top. Quant. Electron. **12**, 431 (2006).
[27] S. V. Zhukovsky, Phys. Rev. A **81**, 053808 (2010).
[28] Computer code MODE SOLUTIONS 4.0 (Lumerical Solutions, Vancouver, British Columbia, Canada, 2010).
[29] L. G. Helt, E. Y. Zhu, M. Liscidini, Li Qian, and J. E. Sipe, Opt. Lett. **34**, 2138 (2009).
[30] Z. Yang, M. Liscidini, and J. E. Sipe, Phys. Rev. A **77**, 033808 (2008).
[31] P. Abolghasem and A. S. Helmy, IEEE J. Quant. Electron. **45**, 646 (2009).
[32] T. E. Kiess, Y. H. Shih, A. V. Sergienko, and C. O. Alley, Phys. Rev. Lett. **71**, 3893 (1993).
[33] T. S. Humble and W. P. Grice, Phys. Rev. A **77**, 022312 (2008).
[34] R. Krischek, W. Wieczorek, A. Ozawa, N. Kiesel, P. Michelberger, T. Udem, and H. Weinfurter, Nature Photon. **4**, 170 (2010).
[35] A. Zavatta, S. Viciani, and M. Bellini, Laser Phys. Lett. **3**, 3 (2006).
[36] P. Abolghasem, M. Hendrych, X. Shi, J. P. Torres, and A. S. Helmy, Opt. Lett. **34**, 2000 (2009).
[37] C. E. Kuklewicz, F. N. C. Wong, and J. H. Shapiro, Phys. Rev. Lett. **97**, 223601 (2006).